ECOLOGY LETTERS

Ecology Letters, (2016) **19**: 450–459 doi: 10.1111/ele.12580

LETTER

Eco-evolutionary dynamics in a coevolving host–virus system

Jens Frickel,[1] Michael Sieber[2] and Lutz Becks[1]*

[1]*Community Dynamics Group, Department Evolutionary Ecology, Max Planck Institute for Evolutionary Biology, 24306 Plön, Germany*

[2]*Institute of Biochemistry and Biology, Universität Potsdam, D-14469 Potsdam, Germany*

**Correspondence: E-mail: lbecks@evolbio.mpg.de*

Abstract

Eco-evolutionary dynamics have been shown to be important for understanding population and community stability and their adaptive potential. However, coevolution in the framework of eco-evolutionary theory has not been addressed directly. Combining experiments with an algal host and its viral parasite, and mathematical model analyses we show eco-evolutionary dynamics in antagonistic coevolving populations. The interaction between antagonists initially resulted in arms race dynamics (ARD) with selective sweeps, causing oscillating host–virus population dynamics. However, ARD ended and populations stabilised after the evolution of a general resistant host, whereas a trade-off between host resistance and growth then maintained host diversity over time (trade-off driven dynamics). Most importantly, our study shows that the interaction between ecology and evolution had important consequences for the predictability of the mode and tempo of adaptive change and for the stability and adaptive potential of populations.

Keywords

Algae-virus, arms race, coevolution, eco-evolutionary dynamics, fluctuating selection, host–virus, infectivity, resistance, trade-off.

Ecology Letters (2016) **19**: 450–459

INTRODUCTION

Theoretical and empirical studies have shown that adaptive variation in ecological relevant traits can lead to evolutionary changes sufficiently rapid to alter the temporal dynamics of populations which in return can alter the evolutionary dynamics (Thompson 1998; Yoshida *et al*. 2003; Duffy & Sivars-Becker 2007; Post & Palkovacs 2009; Ellner *et al*. 2011; Becks *et al*. 2012; Hiltunen *et al*. 2015). The simultaneous changes in ecological and evolutionary properties (eco-evolutionary dynamics) have important consequences for population and community dynamics, ecosystem structure and functioning, and the generation and maintenance of genetic variation and stability (Pelletier *et al*. 2009; Becks *et al*. 2010; Schoener 2011; Koch *et al*. 2014). Despite the large interest in eco-evolutionary dynamics, the entanglement of ecology and evolution has not explicitly been tested with antagonistic coevolving populations, although theoretical predictions and indirect empirical evidence exists (Thompson 1998, 2005; Bohannan & Lenski 2000; Pelletier *et al*. 2009; Hiltunen & Becks 2014).

Antagonistic coevolution has been shown to drive trait and genetic diversity within host and parasite populations (Brockhurst *et al*. 2004, 2014; Best *et al*. 2009; Koskella & Brockhurst 2014). As reciprocal evolutionary changes in antagonistic coevolving populations can be relatively fast and change the ecological interactions simultaneously (Thompson 1998; Hiltunen & Becks 2014), antagonistic coevolution can generate continuous interactions between ecological and evolutionary processes, indicating an important role for eco-evolutionary dynamics. Theoretical models suggest that coevolution needs to be studied in the context of ecology to fully understand whether and how diversity is generated and maintained (Best *et al*. 2009, 2010; Boots *et al*. 2009, 2014). Although the theoretical predictions on coevolutionary dynamics have been tested in several systems [e.g. see examples in Brockhurst & Koskella (2013)], an interaction with ecological dynamics has typically not been shown beyond changes in species interaction strength. There are only a few empirical tests for how the interaction between ecology and evolution can affect coevolution and trait diversity over time, and how these changes in return affect the ecological dynamics. Previous studies discussed for example how smaller population sizes lower the supply of mutations or strength of selection and thus alter coevolution of bacteria and phage (Gómez & Buckling 2011; Friman & Buckling 2013). Considering the short generation times of only a few hours of these organisms and their strong species interactions, sampling intervals spanning several days reduces, however, the power to link the ecological and evolutionary changes. As an example, hosts and their consumer populations can decrease to very low population sizes and increase again within just a few hours. Bottlenecks and their impact on the coevolutionary dynamics might be missed or largely underestimated when sampling with too small time intervals.

Generally, two distinct patterns of host–parasite coevolution are commonly observed during experimental evolution with microbes called arms race dynamics (ARD) or fluctuating selection dynamics (FSD) (Gandon *et al*. 2008; Hall *et al*. 2011; Betts *et al*. 2014; Brockhurst *et al*. 2014; Buckling and Rainey 2002). When hosts (or virus) evolve, increasingly broader resistance (infectivity) ranges over time, coevolutionary dynamics are characterised by an arms race between host and virus (ARD) resulting from directional selection imposed by each antagonist. In contrast, different host (virus) genotypes can alternate in frequency over time, tracking the rarest (most common) genotype of the antagonist. In this case, there is no directional change in resistance (infectivity) range as evolution is driven by frequency dependent selection (fluctuating selection dynamics: FSD). These coevolutionary dynamics

– pure ARD and FSD – can be seen as two extremes of a continuum (Gandon *et al.* 2008; Hall *et al.* 2011). It is not expected that coevolution is consistently driven by one type of dynamics only. For example, the change from one coevolutionary dynamic to another has been observed in prokaryotic experimental systems with multiple coevolutionary cycles and was typically attributed to increasing fitness costs associated with ARD (Brockhurst *et al.* 2004; Hall *et al.* 2011; Koskella & Brockhurst 2014) or to resource availability (Gómez & Buckling 2011; Lopez Pascua *et al.* 2014). Thus, it is likely that the type of coevolutionary dynamics is context dependent. As a consequence, any ecological property or process – such as changes in population size – will be important in these coevolving systems (Brockhurst *et al.* 2004, 2006; Lopez-Pascua & Buckling 2008; Koskella & Brockhurst 2014), as they can alter, for example, associated fitness costs or strength of infection, making it necessary to study antagonistic coevolution in the context of ecology.

From previous observations and theoretical work, there are at least four clear predictions on how coevolution and populations dynamics are linked in antagonistic coevolving species: (1) rapid changes in population sizes of host and parasite are a function of exploitation efficiency of the parasite, that is, the evolution of host resistance and parasite infectivity, (2) density changes affect the rate of infections, which in turn is an important component for the strength of selection, and that these links between ecology and evolution are altered over time by (3) associated fitness costs of resistance and infectivity and (4) population densities, as they determine the supply of new adaptive mutations within populations and affect genetic drift. There is empirical evidence for some of these predictions (e.g. Lenski & Levin 1985; Poullain *et al.* 2008; Gómez & Buckling 2011; Hall *et al.* 2011; Friman & Buckling 2013), but these predictions have not been tested comprehensively within one study, only supported indirectly and as outlined above, not on a sufficient timescale.

In order to establish a comprehensive understanding of how ecological and evolutionary processes together determine the trajectories and outcome of antagonistic coevolving species, we established a novel experimental eukaryotic host–virus system. We used a host–virus system with the asexual reproducing alga *Chlorella variabilis* and a lytic dsDNA virus of the *phycodnaviridae* family (Chlorovirus strain PBCV-1) in continuous cultures. Three replicated continuous cultures (chemostats) of isogenic algae were inoculated with an isogenic strain of the virus, whereas three chemostats remained without virus and served as controls. Algal and virus densities were assessed daily over a period of 3 months and additional time-shift experiments (Gaba & Ebert 2009) allowed us to follow coevolutionary changes in algal host and virus. Individual growth rate assessments of all algal hosts used for the time-shift experiment provided insights into fitness related costs associated with the evolutionary changes. We further explored the ecological and evolutionary dynamics and the underlying mechanisms comparing results from a mathematical model and the chemostat experiments.

Overall, our results show the tight link between coevolutionary changes and ecological population dynamics confirming the outlined predictions. Our study is the first to comprehensively demonstrate how the increase of resistance range coincides with an increase in growth costs, how ARD switch to trade-off driven dynamics (TDD) due to evolutionary constraints in the virus, how the types of coevolution corresponded to different population dynamics, and how the costly resistance of the host stabilised host and virus population dynamics while less resistant and general resistant hosts cycled over time.

MATERIALS AND METHODS

Chemostat experiments

Experiments were performed in continuous flow-through systems (chemostats) with a modified version of bold's basal medium. One isolated algal clone was used to start all six chemostats in order to minimise the initial genetic variability. Three out of six chemostats were inoculated with purified and concentrated virus at day 12. Virus (Brussaard 2004) and alga densities were counted daily. Samples of virus and alga populations were stored every second day by plating algae on BBM agar plates and storing virus at 4 °C (Van Etten *et al.* 1983) after filtering (0.45 μm cellulose syringe filter; Supporting Information).

Time-shift experiments

To examine the evolution of resistance and infectivity of algae and virus, eleven time-points (Grey vertical lines: Fig. 1) per chemostat were selected. For each time-point, ten individual host clones were randomly isolated from the agar plates and re-grown in batch cultures (11 time-points × 10 clones per time-point = total of 110 clones per replicated chemostat). Each host clone was exposed to each virus population separately; to the virus population from the same time-point from which the host clones were isolated, to each virus population from time-points from their relative past and to each virus population from time-points from their relative future (110 host clones × 11 time-points = 1210 combinations per chemostat). All algal clones were individually assayed as resistant or susceptible to a particular virus population by comparing growth rates of alga clones exposed to virus, to growth rates of the same alga clone without the virus. For each alga-virus combination, algae and virus were diluted to equal densities resulting in MOI of 0.01 particles/algal cell. Four technical replicates per combination were incubated in 96 well plates and maintained in continuous light. Growth rates were calculated based on ODs (Tecan, Infinite M200PRO, 680 Männedorf, Switzerland) measured at 0 hours and after 72 h. To assess whether the algal clones were resistant or susceptible to a particular virus population, we compared the mean growth rate plus 2 standard deviations of the four technical replicates to the mean growth rate minus 2 standard deviations of the control (growth without virus).

Data analysis

All data analyses were performed in Rstudio (Rstudio 2014) and R (RCoreTeam 2014) using the lme4 (Bates *et al.* 2014)

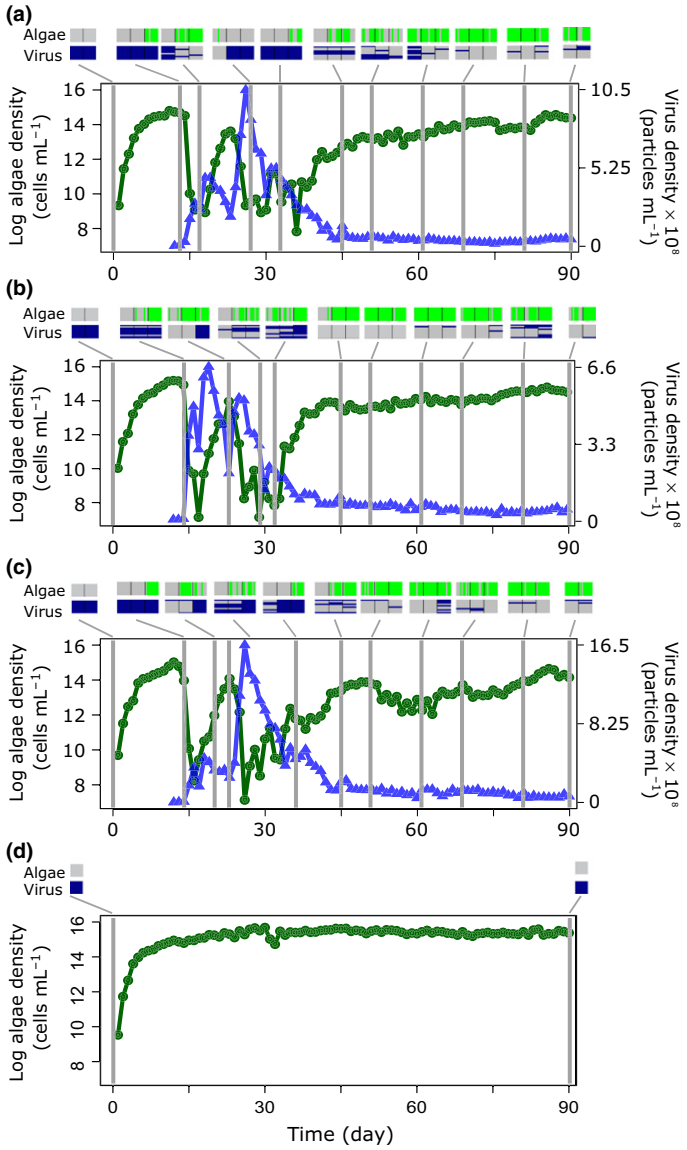

Figure 1 Coevolutionary and population dynamics of algae-virus (a–c) and algae chemostats (d). Green (dots): algal densities (natural logarithm); blue (triangles): virus densities. Grey vertical lines indicate days of time-shift experiments. Colour coded squares above grey lines show alga evolution and virus evolution. The algae squares represent susceptibility assays of algae from one time-point in the past (first square), contemporary time-point (second square) and one time-point in the future (third square) to the contemporary virus population. Similarly, virus squares represent infectivity essays of virus from one time-point in the past (first square), the contemporary time-point (second square) and one time-point in the future (third square) to contemporary algae. Algae: grey = susceptible to virus; green = resistant to virus. Virus: grey = unable to infect algae; blue = able to infect algae. Ten algal clones per time-point were tested against the whole virus population per time-point.

and multcomp (Hothorn *et al.* 2008) packages. Densities of host populations (last day) were compared between alga-virus and control chemostats using student's t test (unpaired and equal variance) after confirming equal variances between samples (F test to compare variances: $F_{2,2} = 5.852$, $P = 0.29$). Host resistance ranges were calculated for each individual host clone by calculating to how many virus populations (from their relative past, present and future) a host clone was resistant. As each host clone was exposed separately to each virus population used for the time-shift experiment (11 in total), the maximum resistance range is 11 (general resistant host). Thus, a general resistant host is resistant to all virus populations (from all time-points) from their chemostat. Virus infectivity ranges were calculated as how many host clones out of 110 clones (10 clones per time-point × 11 time-points per replicate) could be infected by a particular virus population. Average values were normalised to maximum infectivity.

We divided resistance and infectivity data from the time shift experiment into two periods: until a general resistant host was first observed (Fig. 1a: days 13–45, Fig. 1b: 14–32, Fig. 1c: 14–51; ARD in Fig. S1) and all later time-points (Fig. 1a: days: 51–90, Fig. 1b: 45–90, Fig. 1c: 61–90; TDD, see below; Fig. S1). We calculated for every host clone the proportion of virus populations from their relative past, present and future (virus time-shift) the clone was resistant to. The virus populations used to calculate these proportions were restricted to the same period from which the host was isolated (ARD or TDD period; Fig. S1). If coevolution was driven by ARD, we expected that hosts are highly resistant to all virus populations from their relative past (within the period from which the host was isolated; Fig. S1), and not resistant to all virus populations from their relative future (within the period from which the host was isolated; Fig. S1). As such, virus time-shift should be significant for host resistance and resistance should be significantly different between future (low resistance) and past (high resistance) virus time-shifts. To test this, we used a generalised linear model (GLM, quasi-binomial errors) with resistance proportions per algal clone (as response) across virus time-shift and compared this model to a null-model. We performed the same analysis to test whether host time-shift was significant for virus infectivity. Resistance between virus time-shift was further compared using multiple comparisons of means with Tukey contrasts. Looking for selective sweeps, hosts were assigned to distinct resistance types based on unique resistance-profiles (Fig. S1) during the ARD period with one time-point extra (to be able to track sweep of general resistant hosts) and time-point zero left out (as the host and virus were not yet exposed in the chemostats to each other at time zero). Rates of coevolution were calculated from slopes for the proportion of hosts resistant to virus from one time point in the past, contemporary and in the future (Brockhurst *et al.* 2003). We used mixed effect models with MOI (proxy for force of infection) and type of dynamic (ARD or TDD) as fixed, and replicate as random effect to test for a correlation between rates of coevolution and infection strength.

Host per capita growth rates were obtained from growth rates of individual host clones growing without the virus. We used linear mixed models (LMM) to test for a correlation between per capita growth rates and host resistance range (resistance range as fixed effect and replicated chemostat as random effect). We tested for a correlation between host population growth rates (obtained from population dynamics) and proportion of resistant host clones (resistant to contemporary virus) using LMM (proportion of resistant host clones as fixed effect and replicated chemostat as random effect). A

selection coefficient was estimated for each time-point used in the time-shift experiment by: $s_p = 1 -$ [growth of algae in the presence of the contemporary virus/growth of algae]).

Mathematical model

We modeled both the population dynamics and coevolution of algae and virus with a fully dynamical eco-evolutionary model using a modified gene-for-gene infection mechanism (Forde *et al.* 2008). The modified gene-for-gene interaction implies that virus type P_i could infect host type B_j if and only if $i \geq j$. We assumed N host types and $N-1$ virus types, implying that host type B_N is generally resistant (Fig. S2). We modeled the coevolutionary interactions of algae $B = (B_1, \ldots, B_N)$ and virus $P = (P_1, \ldots, P_{N\text{-}1})$ in a chemostat environment with continuous inflow of resources and outflow. Host resistance was costly, i.e. host growth rate declined with increasing resistance range. Host and virus evolved by mutations that altered resistance range and host range. We assumed that evolution progressed step-wise, i.e. B_i could mutate into B_{i+1} or reverse to B_{i-1}. For model detailed description, see Supporting Information.

RESULTS

Population dynamics

We observed two distinct patterns in the population dynamics of host and virus; host and virus populations oscillated for the first ~ 45 days, followed by a more stable period with slowly increasing host populations and low virus densities (Figs 1 and 2). In the experiments, cycle amplitudes decreased very rapidly during the first period and the second host maximum (~ day 32) was not observed in all replicates (Fig. 1). Model results also showed oscillations initially but oscillations were not damped as in the experiments (Fig. 2). The control chemostats with only algae showed stable densities (without oscillations) after initial increase to high densities (Fig. 1d). However, host densities in the algae-virus chemostats during the stable period were well below the stable algal densities observed in control chemostats (Fig. 1, Fig. S3; independent t test: $t = 4.95$, d.f. = 4, $P = 0.0078$).

Coevolutionary dynamics

Using time-shift experiments, we tested whether and when hosts evolved resistance to the virus, and whether and when the virus evolved counter adaptations in return. An infection matrix summarising the time-shift data (Fig. S1) shows that susceptible host clones were replaced by resistant host clones at later time-points when tested against the same virus population (black arrows, Fig. S1). Similarly virus populations that could not infect the host were replaced at later time-points by virus populations that were able to infect previously resistant hosts (red arrows, Fig. S1). Thus, we found that algae and virus populations coevolved rapidly and observed 2–3 cycles of hosts evolving resistance (black arrows, Fig. S1), and 1–2 cycles of virus evolving counter-adaptations to infect previously resistant hosts (red arrows, Fig. S1). As experiments were started isogenically, resistance and infectivity evolved *de novo*. Coevolution resulted in an initial rapid increase in virus infectivity and host resistance ranges (Fig. 3, Fig. S4). Host resistance range reached its maximum when a general resistant host evolved around days 32–51 (Fig. 3, arrows). Generalist hosts could not be infected by any virus population from any time-point, suggesting that the virus was evolutionary constrained and unable to overcome the general resistance mechanism of the host (virus infectivity did not reach its maximum in any replicate; Fig. S4). Importantly, this constraint was not related to low encounter rates, as MOI values (multiplicity of infection) remained high (Fig. S5). Algae isolated from the end point of control chemostats did not evolve any resistance against the ancestral virus (Fig. 1d), confirming that evolution of resistance resulted solely from the algae-virus interactions.

The initial coevolutionary dynamics were consistent with ARD, i.e., until the time-point when the generalist resistant host evolved. All host clones (for ARD-period; Fig. S1) from past time-points relative to the virus were highly susceptible to that virus population (Fig. 4a, Figs S6a, S7), but all host clones from future time-points relative to virus were highly resistant to that virus population. A generalised linear model showed that host time-point (past, contemporary, future) was significant for host resistance during the ARD period (GLM, $F_{2,36}$=25.649, $P = 1.19e^{-7}$) and resistance was significantly different between past, contemporary and future time-points (Tukey mcp; past-future: $P < 0.001$, contemporary-future: $P = 0.003$, past-contemporary: $P = 0.0014$). Likewise, all virus populations (for ARD-period) from past time-points relative to the host population had low infection success, but virus populations from future time-points were highly infective (Fig. 4c, Figs S6b, S8; GLM, $F_{2,36} = 17.238$, $P = 5.61e^{-6}$, Tukey mcp; past-future: $P < 0.001$, contemporary-future: $P = 0.017$, past-contemporary: $P = 0.13$). These patterns were consistent with ARD, where hosts (virus) evolve greater resistance (infectivity). Moreover, hosts that acquired resistance to a particular virus type stayed resistant to all previous viruses, whereas all virus populations were able to infect previous susceptible algal types (Fig. S1). Thus, ARD resulted from directional selection for increasing host resistance and virus infectivity range. ARD with directional selection typically result in selective sweeps (Brockhurst *et al.* 2014). Our data do indeed show consecutive appearance of distinct resistant host types followed by rapid increases to high frequency or temporal fixation (Fig. 5).

The coevolutionary dynamics changed after a general resistant host emerged; ARD stopped and host (virus) time-point was not significant for resistance (infectivity) (Fig. 4b,d, Figs. S7, S8, GLM, $F_{2,36} = 1.82$, $P = 0.18$; $F_{2,36} = 1.12$, $P = 0.89$). Furthermore, we found that the generalist host did not go to fixation but that less resistant host types (resistant to different virus types and to a different number of virus types) coexisted with the generalist (Fig. 3). A significant cost was associated with host resistance in terms of reduced per capita growth rates (Fig. 6a, Fig. S9). Growth rates decreased with increasing host resistance range (LME: $\chi^2 = 93.90$, d.f. = 1, $P < 2.2e^{-16}$), showing that costs accumulated with evolving resistance to increasingly more virus types. Consequently, the general resistant host had the lowest per capita growth rate.

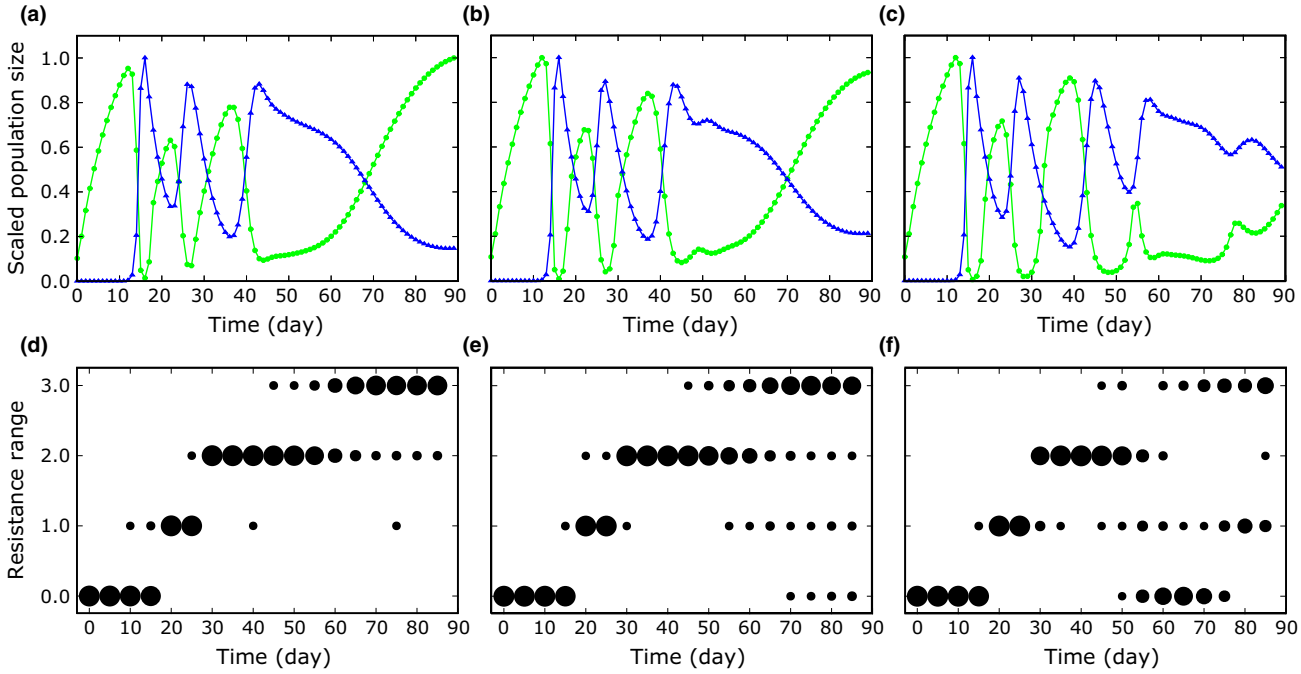

Figure 2 Population dynamics (a–c) and host resistance range (d–f) resulting from models with different host trade-off values. (a–c) population densities are scaled to maximum density of algae or virus. Green (dots): algal densities; blue (triangles): virus densities. (d–f) Host resistance range was calculated as the number of virus types to which an algal clone is resistant. Size of the dots correspond to the number of host clones (1–10) with a certain resistance range (10 random clones per time-point were sampled from the populations). (a, d) Model results without trade-off; (b, e) model results with experimentally observed trade-off; (c, f) model results for strong trade-off (see Material and Methods and Supporting Information).

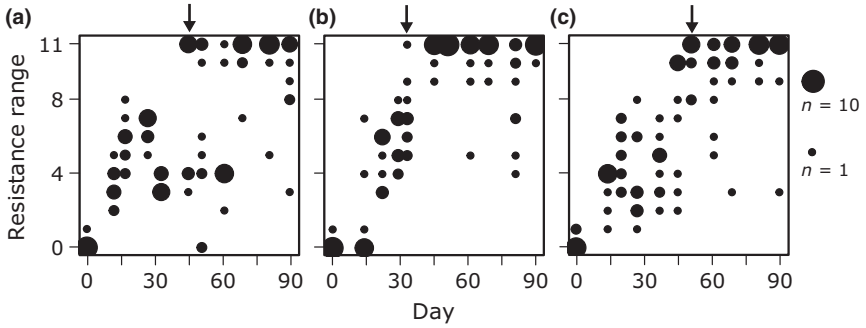

Figure 3 Evolution of host resistance range in chemostat experiments. Resistance range calculated as number of virus populations (from all time-points) to which an algal clone is resistant. Host resistance range increases over time from no resistance (0) to a general resistant type (=11; resistant to all virus populations; first occurrence of general resistant host type is indicated by arrows on top). (a–c) Replicates corresponding to Fig. 1a–c. Size of the dots correspondent to number of host clones (1–10). Every replicate (a–c) shows the 11 time-points from which hosts were isolated.

Model results and trade-off

To better understand the shift in ecological and evolutionary dynamics and the underlying mechanisms we used a mathematical model of a host-virus chemostat system. Specifically, we tested for the role of the resistance-growth trade-off and followed population and evolutionary dynamics assuming three different scenarios with different trade-off strengths (SI). Overall, we found two distinct periods over time similar to our experimental data. Before the generalist evolved, host-virus populations cycled and evolution was characterised by ARD; after the generalists' emergence, population dynamics became more stable (host increasing, virus decreasing to low densities) and evolutionary dynamics changed, depending on the strength of the trade-off considered. When there was no trade-off (Fig. 2a, d, Fig. S10a,b), the general resistant type almost reached fixation and only one other host type was maintained (when using similar sampling as in experiments, Fig. 2d), but only due to mutations. Assuming the trade-off we observed in the experiments, the general resistant type dominated (Fig. 2b,e, Fig. S10c,d) but several different other host types coexisted. Increasing the costs of resistance further led to even higher levels of diversity maintained (Fig. 2c,f, Figs S10e,f, S11). Overall, the presence of the generalist stabilised host-virus population dynamics as observed in the experi-

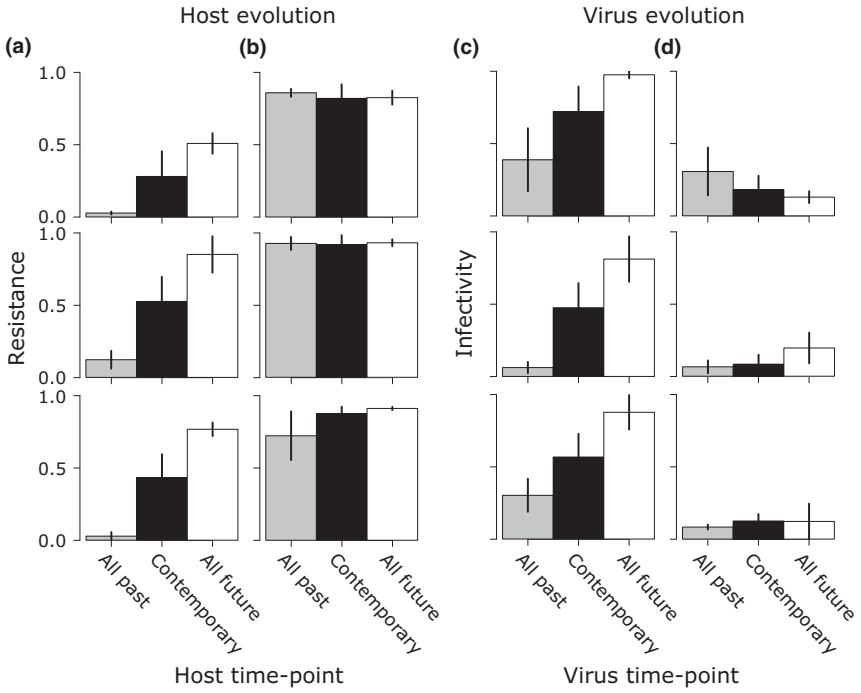

Figure 4 Coevolutionary dynamics in algal-virus populations in chemostats. (a) Average resistance of host clones (fraction of host clones that were resistant ± SE) exposed to virus populations during ARD-period and (b) TDD-period. (c) Average infectivity of virus populations (fraction of host clones that could be infected ± SE) during ARD-period and (d) TDD-period. (a, b) Contemporary are host and virus combinations from the same time-point, all past are combinations of hosts from all previous time-points with the virus populations and all future are combinations of hosts from all further time-points with the virus populations. (c, d) Contemporary are virus and host combinations from the same time-point, all past are combinations of virus populations from all previous time-points with the host, all future are combinations of virus populations from further time-points with the host. (a, c) Data show clear arms race dynamics as time-point is significant for host resistance and virus infectivity.

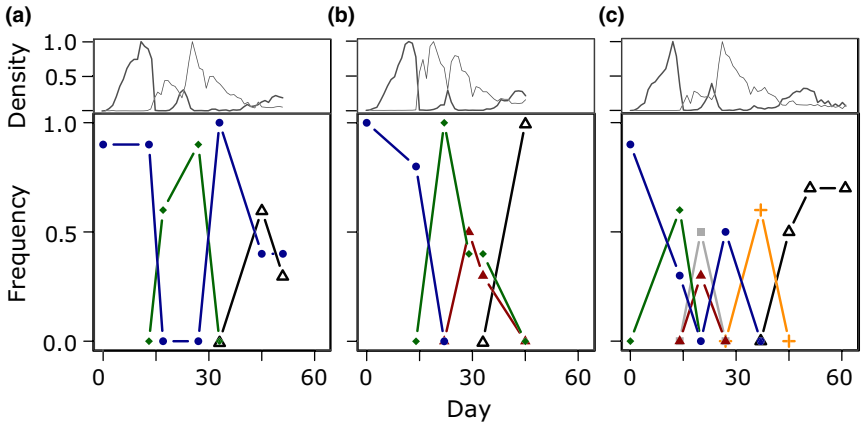

Figure 5 Frequencies of resistance host types over time from chemostat experiments. Frequencies of distinct resistant host types during ARD (until generalist) are shown in different colours and symbols. Blue (dots) are initial not-resistant hosts. Only distinct resistant types with frequencies higher than 0.2 are shown. Scaled population dynamics (density) of host (bold grey line) and virus (thin grey line) are shown above each frequency plot as densities scaled to the maximum population size. (a–c) correspond to Fig. 1.

ments, but the rate at which host increased while virus population size decreased depended on the diversity of host types. Finally, we simulated the dynamics with the experimentally observed trade-off for 360 days (Fig. S12). Here, diversity was maintained while the general resistant host remained at high frequencies and frequencies of host types with lower resistant ranges changed over time while population densities showed only small fluctuations.

Eco-evolutionary dynamics

Overall, host population growth was positively correlated with the fraction of resistant host clones in the population (LME: $\chi^2 = 31.88$, d.f. = 1, $P < 0.001$; Fig. S13). Furthermore, changes in host susceptibility and virus infectivity correlated with distinct changes in population sizes (Fig. 1); host populations decreased when they were susceptible to the contempo-

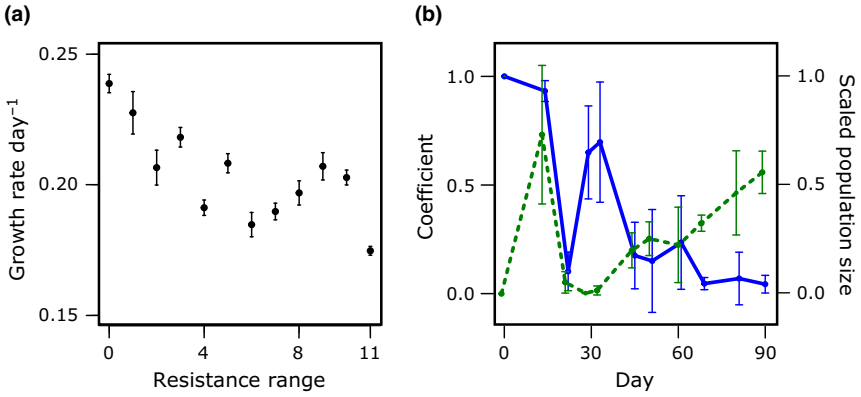

Figure 6 Evolution of trade-off and eco-evolutionary dynamics in chemostats. (a) Trade-off between host resistance range and average per capita growth rate (± SEM). (b) Changes in selection coefficient (blue solid line, ± SD) and algal census population size (green dotted line, ± SD). For all $n = 3$.

rary virus population (e.g. Fig. 1c, day 14) and increased when hosts were resistant to the contemporary virus (e.g. Fig. 1c, day 20). Thus, the reciprocal antagonistic changes through *de novo* evolution of resistance and infectivity constantly changed the ecological effect of the two antagonists. Rates of coevolution were significant different for the ARD and TDD period (LME: type of dynamic: $\chi^2 = 11.85$, d.f. = 2, $P = 0.003$; type of dynamic × MOI: $\chi^2 = 5.38$, d.f. = 1, $P = 0.02$), but we did not observe a correlation between force of infection and rates of coevolution (LME: MOI: $\chi^2 = 5.39$, d.f. = 2, $P = 0.068$, Fig. S14). We further observed that selection and *census* population size N of the host varied over time (Fig. 6b). In particular, the population size of the host was reduced to very low numbers (~ 1000 cells mL^{-1}) during ARD, but was large (increasing) when ARD ended. Selection by the virus cycled during the ARD period, but was low during the TDD period. Thus, there were time-points when s_p and N were small, time-points when s_p and N were high and time-points with one high, the other low.

In a model without evolution the virus rapidly decreased host densities (until the end of the simulated time, Fig. S15) and the lack of further population growth indicated that populations were unable to recover without evolutionary change and underlines the important link between evolution and ecology.

DISCUSSION

We experimentally studied eco-evolutionary dynamics in coevolving host-virus systems and combined our analysis with a corresponding mathematical model. Host and virus densities showed damped oscillations for the first half of the experiment and stabilised hereafter with host densities remaining well below densities observed in control chemostats. Algae and virus coevolved through ARD initially and we observed selective sweeps of new resistant host types. ARD ended with the asymmetrical evolution of a general resistant host, which did not go to fixation due to a trade-off between host-resistance and growth. We thus refer to these dynamics as TDD. Interestingly, the frequencies of the more susceptible types changed over time.

Besides the maintenance of diversity, theory and empirical studies suggest that trade-offs are important for the type of antagonistic coevolution (Sasaki 2000; Hall *et al.* 2011; Lopez Pascua *et al.* 2014). A trade-off can limit the evolution of an ever-increasing host (virus) resistance (infectivity) range as costs accumulate with increasing amounts of resistance (infectivity) alleles. The accumulating cost of resistance would restrain the evolution of a general resistant (infective) host (virus) as the trade-off weakens their response to directional selection leading eventually to a shift from ARD to FSD. In our study, the trade-off had no direct consequences for the evolutionary outcome during ARD. The trade-off did not limit the host's ability to respond to directional selection as we observed the evolution of a general resistant host in all replicate chemostats. Model analysis confirmed that ARD ended only after the evolution of a general resistant host. Furthermore, the model showed that evolutionary and population dynamics during ARD assuming no trade-off (Fig. 2a,d) were almost identical to model results with the experimental trade-off, indicating that the trade-off was indeed less important here.

Our study shows strong links between ecology and evolution. These eco-evolutionary dynamics are evident from several observations. First, we observed that host population growth depended on the fraction of resistant hosts in the population. Second, the appearance of newly resistant host types was clearly reflected in the population dynamics of both alga and virus (Fig. 5). The evolution of new host (or virus) types affected the ecological interaction strength between the antagonists, and lead to changes in population dynamics (one antagonist increased in density, the other one decreased). The changes in population densities then altered directional selection strength, resulting in further evolutionary change, and so on. As a result, the population dynamics of hosts and virus showed damped oscillations during ARD (sustained oscillations in the model). This interaction between ecology and evolution continued until a general resistant host appeared and ARD ended. A third link between ecology and evolution was observed when the population dynamics stabilised during TDD. Here, virus densities decreased to low values, while host densities increased. From this point on, host populations had high resistance on average (Fig. 4b) as the general resistant host reached high frequencies and no further population cycles were observed in the experiments. Thus, the evolution

of a general resistant host stabilised population dynamics. Here, the trade-off became important for the maintenance of (host) diversity. Directional selection for resistance weakened (due to low virus densities) and higher host densities strengthened intraspecific competition between faster growing but more susceptible and general resistant hosts. Model analysis showed indeed that the amount of diversity maintained depended on the strength of the trade-off (Fig. 2, Figs. S11, S12). The trade-off had further consequences, as lower per capita growth rates of resistant host cells (which dominated the host population) resulted in lower host population densities (during TDD) compared to control chemostats. Thus, population size changes can immediately alter interspecific and intraspecific interaction strength, whereas population size depends on the coevolutionary state or history and changes within a few generations.

The eco-evolutionary dynamics had considerable further consequences for our understanding of the dynamics of two coevolving antagonists. Although the population and evolutionary dynamics were relatively similar between experimental replicates, differences in *census* population size (ecology) and selection (evolution) over time (Fig. 6b) likely played a considerable role for the timing and emergence of novel adaptive mutations. For example, the generalist host appeared first at different time-points (Fig. 3: day 33, 45, 51) and we observed differences in appearance and increase in distinct resistant host types between the replicated chemostats (Fig. 5). These observations indicate that changes in population size and selection can weaken or strengthen stochastic effects during reciprocal adaptations as predicted by theory (Gokhale *et al.* 2013). Although we find that coevolution during the first half of the experiment was driven by ARD, average resistance of hosts from further time-points (relative to virus population) was not complete in all replicates (Fig. 4a). This observation resulted from a less resistant host type that re-emerged in two out of three replicates (Fig. 5a,c), which is not predicted under pure ARD. During these periods, host densities were very low, potentially resulting in slower emergence of novel mutations. Together with the random loss of genotypes (drift) and the lack of novel mutations, ARD temporary softened (i.e., moved towards FSD like dynamics). As no host type was resistant to the virus at that time, the ancestral not-resistant host type invaded the host population again. Interestingly, this non-resistant host type had the highest growth rate and thus was able to out-compete hosts with higher resistance ranges. These results indicate that, as soon as hosts could not respond to directional selection imposed by the virus, the trade-off determined the dominating host type. However, when new adaptive mutations emerged, coevolution could again continue through ARD. Indeed, we found that MOI (as proxy for force of infection and selection) was not significantly correlated with the rate of coevolution, confirming that coevolution depended not only on infection strength but on the supply of mutations, drift and the trade-off as well.

Our study also synthesises several previous results and predictions into a coherent picture. Similar to studies with prokaryotic systems, we found a shift from ARD to FSD (Gómez & Buckling 2011; Hall *et al.* 2011), although the underlying mechanism was different here (TDD) and previous studies did not link evolutionary dynamics to detailed temporal changes in population sizes. Furthermore, other studies discovered asymmetrical coevolution between host and virus, which can impede extensive coevolution (Lenski & Levin 1985), but can lead nonetheless to multiple rounds of coevolution (Poullain *et al.* 2008; Hall *et al.* 2011) as in our study. Lenski & Levin (1985) also showed the stabilisation of population dynamics during FSD and suggest the maintenance of host diversity through a trade-off as we have found here. A stabilising effect of rapid evolution has also been demonstrated in studies on eco-evolutionary dynamics (Becks *et al.* 2010) but they did not consider coevolution between consumer and resource population. Overall our detailed analysis goes beyond previous studies by showing that the dynamic effect of selection and population size is an inherent part of eco-evolutionary dynamics, with important implications for the evolutionary dynamics.

CONCLUSION

Viruses have been shown to play an important role in termination of algal blooms (Fuhrman 1999; Brussaard *et al.* 2005), affect nutrient and energy cycling (Suttle *et al.* 1990; Suttle 2007; Haaber & Middelboe 2009) and plankton community structure (Suttle 2007; Short 2012). Our experiment showed rapid recovery of algal populations through the evolution of general resistance, finally reducing the effect of virus on algal mortality.

We showed here the important entanglement of ecology and evolution in antagonistic coevolving. Coevolution affected population density and both densities and evolution then in return, resulted in further evolutionary changes, and so on. Although the fitness-associated costs of resistance did not alter coevolution itself as the switch from ARD to TDD resulted from an evolutionary constraint in the virus, they determined the host population sizes and maintenance of variation during TDD. Our data indicate that low population densities affected coevolutionary dynamics through mutation supply and/or drift as we observed softening of the ARD. Overall, the outcome and trajectory of coevolution with subsequent effects on the ecological dynamics and community structure were determined by many factors, which are intertwined and operate on same timescales (Fig. S16). As such, the eco-evolutionary dynamics have important consequences for stability of populations and genetic diversity of populations, as well as how selection and demography affect evolutionary trajectories.

ACKNOWLEDGEMENTS

We are grateful to James Van Etten for providing us with the algal and virus cultures and Julia Haafke for helping with the data collection. Our thanks to A. Binzer, P. Feulner, N. Hairston Jr. and Teppo Hiltunen for helpful comments on a previous version of the manuscript.

AUTHORSHIP

J.F and L.B. conceived and designed the study, J.F. performed experiments, M.S. developed and analysed the model,

J.F., M.S. and L.B. analysed the results and wrote the paper.

REFERENCES

Bates, D., Maechler, M., Bolker, B.M. & Walker, S. (2014). *Linear Mixed-effects Models using Eigen and S4, R Package Version 1.1-7*. *J. Stat. Softw.*, 67(1), 1–48. doi:10.18637/jss.v067.i01.

Becks, L., Ellner, S.P., Jones, L.E. & Hairston, N.G. (2010). Reduction of adaptive genetic diversity radically alters eco-evolutionary community dynamics. *Ecol. Lett.*, 13, 989–997.

Becks, L., Ellner, S.P., Jones, L.E. & Hairston, N.G. (2012). The functional genomics of an eco-evolutionary feedback loop: linking gene expression, trait evolution, and community dynamics. *Ecol. Lett.*, 15, 492–501.

Best, A., White, A. & Boots, M. (2009). The implications of coevolutionary dynamics to host-parasite interactions. *Am. Nat.*, 173, 779–791.

Best, A., White, A., Kisdi, E., Antonovics, J., Brockhurst, M.A. & Boots, M. (2010). The evolution of host-parasite range. *Am. Nat.*, 176, 63–71.

Betts, A., Kaltz, O. & Hochberg, M.E. (2014). Contrasted coevolutionary dynamics between a bacterial pathogen and its bacteriophages. *Proc. Natl Acad. Sci. USA*, 111, 11109–11114.

Bohannan, B.J.M. & Lenski, R.E. (2000). Linking genetic change to community evolution: insights from studies of bacteria and bacteriophage. *Ecol. Lett.*, 3, 362–377.

Boots, M., Best, A., Miller, M.R. & White, A. (2009). The role of ecological feedbacks in the evolution of host defence: what does theory tell us? *Phil. Trans. R. Soc. B.*, 364, 27–36.

Boots, M., White, A., Best, A. & Bowers, R. (2014). How specificity and epidemiology drive the coevolution of static trait diversity in hosts and parasites. *Evolution*, 68, 1594–1606.

Brockhurst, M.A. & Koskella, B. (2013). Experimental coevolution of species interactions. *Trends Ecol. Evol.*, 28, 367–375.

Brockhurst, M.A., Morgan, A.D., Rainey, P.B. & Buckling, A. (2003). Population mixing accelerates coevolution. *Ecol. Lett.*, 6, 975–979.

Brockhurst, M.A., Rainey, P.B. & Buckling, A. (2004). The effect of spatial heterogeneity and parasites on the evolution of host diversity. *Proc. R. Soc. B*, 271, 107–111.

Brockhurst, M.A., Fenton, A., Roulston, B. & Rainey, P.B. (2006). The impact of phages on interspecific competition in experimental populations of bacteria. *BMC Ecol.*, 6, 19.

Brockhurst, M.A., Chapman, T., King, K.C., Mank, J.E., Paterson, S. & Hurst, G.D. (2014). Running with the Red Queen: the role of biotic conflicts in evolution. *Proc. R. Soc. B*, 281, 20141382.

Brussaard, C.P.D. (2004). Optimization of procedures for counting viruses by flow cytometry. *Appl. Environ. Microbiol.*, 70, 1506–1513.

Brussaard, C.P.D., Kuipers, B. & Veldhuis, M.J.W. (2005). A mesocosm study of *Phaeocystis globosa* population dynamics – 1. Regulatory role of viruses in bloom. *Harmful Algae*, 4, 859–874.

Buckling, A. & Rainey, P.B. (2002). Antagonistic coevolution between a bacterium and a bacteriophage. *Proc. R. Soc. B*, 269, 931–936.

Duffy, M.A. & Sivars-Becker, L. (2007). Rapid evolution and ecological host-parasite dynamics. *Ecol. Lett.*, 10, 44–53.

Ellner, S.P., Geber, M.A. & Hairston, N.G. (2011). Does rapid evolution matter? Measuring the rate of contemporary evolution and its impacts on ecological dynamics. *Ecol. Lett.*, 14, 603–614.

Forde, S.E., Beardmore, R.E., Gudelj, I., Arkin, S.S., Thompson, J.N. & Hurst, L.D. (2008). Understanding the limits to generalizability of experimental evolutionary models. *Nature*, 455, 220–223.

Friman, V.-P. & Buckling, A. (2013). Effects of predation on real-time host–parasite coevolutionary dynamics. *Ecol. Lett.*, 16, 39–46.

Fuhrman, J.A. (1999). Marine viruses and their biogeochemical and ecological effects. *Nature*, 399, 541–548.

Gaba, S. & Ebert, D. (2009). Time-shift experiments as a tool to study antagonistic coevolution. *Trends Ecol. Evol.*, 24, 226–232.

Gandon, S., Buckling, A., Decaestecker, E. & Day, T. (2008). Host-parasite coevolution and patterns of adaptation across time and space. *J. Evol. Biol.*, 21, 1861–1866.

Gokhale, C.S., Papkou, A., Traulsen, A. & Schulenburg, H. (2013). Lotka-Volterra dynamics kills the Red Queen: population size fluctuations and associated stochasticity dramatically change host-parasite coevolution. *BMC Evol. Biol.*, 13, 254.

Gómez, P. & Buckling, A. (2011). Bacteria-phage antagonistic coevolution in soil. *Science*, 332, 106–109.

Haaber, J. & Middelboe, M. (2009). Viral lysis of *Phaeocystis pouchetii*: implications for algal population dynamics and heterotrophic C, N and P cycling. *ISME J.*, 3, 430–441.

Hall, A.R., Scanlan, P.D., Morgan, A.D. & Buckling, A. (2011). Host-parasite coevolutionary arms races give way to fluctuating selection. *Ecol. Lett.*, 14, 635–642.

Hiltunen, T. & Becks, L. (2014). Consumer co-evolution as an important component of the eco-evolutionary feedback. *Nat. Commun.*, 5, 5226.

Hiltunen, T., Ayan, G.B. & Becks, L. (2015). Environmental fluctuations restrict eco-evolutionary dynamics in predator–prey system. *Proc. R. Soc. B*, 282, DOI: 10.1098/rspb.2015.0013.

Hothorn, T., Bretz, F. & Westfall, P. (2008). Simultaneous inference in general parametric models. *Biom. J.*, 50, 346–363.

Koch, H., Frickel, J., Valiadi, M. & Becks, L. (2014). Why rapid, adaptive evolution matters for community dynamics. *Front. Ecol. Evol.*, 2, 17.

Koskella, B. & Brockhurst, M.A. (2014). Bacteria-phage coevolution as a driver of ecological and evolutionary processes in microbial communities. *FEMS Microbiol. Rev.*, 38, 916–931.

Lenski, R.E. & Levin, B.R. (1985). Constraints on the coevolution of bacteria and virulent phage: a model, some experiments, and predictions for natural communities. *Am. Nat.*, 125, 585–602.

Lopez Pascua, L., Hall, A.R., Best, A., Morgan, A.D., Boots, M. & Buckling, A. (2014). Higher resources decrease fluctuating selection during host-parasite coevolution. *Ecol. Lett.*, 17, 1380–1388.

Lopez-Pascua, L.D.C. & Buckling, A. (2008). Increasing productivity accelerates host-parasite coevolution. *J. Evol. Biol.*, 21, 853–860.

Pelletier, F., Garant, D. & Hendry, A.P. (2009). Eco-evolutionary dynamics. *Phil. Trans. R. Soc. B.*, 364, 1483–1489.

Post, D.M. & Palkovacs, E.P. (2009). Eco-evolutionary feedbacks in community and ecosystem ecology: interactions between the ecological theatre and the evolutionary play. *Phil. Trans. R. Soc. B.*, 364, 1629–1640.

Poullain, V., Gandon, S., Brockhurst, M.A., Buckling, A. & Hochberg, M.E. (2008). The evolution of specificity in evolving and coevolving antagonistic interactions between a bacteria and its phage. *Evolution*, 62, 1–11.

RCoreTeam (2014). *R: A Language and Environment for Statistical Computing*. 3.1.2. 2014, Vienna, Austria. http://www.R-project.org/.

Rstudio (2014). *R-studio: Integrated Development Environment for R. 0.98.1091*. Rstudio, Boston, USA. http://www.rstudio.com/.

Sasaki, A. (2000). Host-parasite coevolution in a multilocus gene-for-gene system. *Proc. R. Soc. B*, 267, 2183–2188.

Schoener, T.W. (2011). The newest synthesis: understanding the interplay of evolutionary and ecological dynamics. *Science*, 331, 426–429.

Short, S.M. (2012). The ecology of viruses that infect eukaryotic algae. *Environ. Microbiol.*, 14, 2253–2271.

Suttle, C.A. (2007). Marine viruses – major players in the global ecosystem. *Nat. Rev. Microbiol.*, 5, 801–812.

Suttle, C.A., Chan, A.M. & Cottrell, M.T. (1990). Infection of phytoplankton by viruses and reduction of primary productivity. *Nature*, 347, 467–469.

Thompson, J.N. (1998). Rapid evolution as an ecological process. *Trends Ecol. Evol.*, 13, 329–332.

Thompson, J.N. (2005). *Geographic Mosaic of Coevolution*. University Chicago Press, Chicago, IL.

Van Etten, J.L., Burbank, D.E., Xia, Y. & Meints, R.H. (1983). Growth cycle of a virus, PBCB-1, that infects chlorella-like algae. *Virology*, 126, 117–125.

Yoshida, T., Jones, L.E., Ellner, S.P., Fussmann, G.F. & Hairston, N.G. (2003). Rapid evolution drives ecological dynamics in a predator-prey system. *Nature*, 424, 303–306.

SUPPORTING INFORMATION

Additional Supporting Information may be downloaded via the online version of this article at Wiley Online Library (www.ecologyletters.com).

Editor, Gregor Fussmann
Manuscript received 2 December 2015
First decision made 31 December 2015
Second decision made 7 January 2016
Manuscript accepted 12 January 2016